

Electrically Controlled Magnetic Memory and Programmable Logic based on Graphene/Ferromagnet Hybrid Structures

Y. G. Semenov, J. M. Zavada, and K. W. Kim

*Department of Electrical and Computer Engineering,
North Carolina State University, Raleigh, NC 27695-7911*

Abstract

It has been shown that the combining of the electrical effect on the exchange bias field with giant magneto-resistance effect of the graphene/ferromagnet hybrid structures reveals a new non-volatile magnetic random access memory device conception. In such device an electric bias realizes the writing bits instead a magnetic field of remote word line with high energy consumption. Interplay of two graphene mediated exchange bias fields applied to different sides of free ferromagnet results in programable logic operations that depends on specific realization of the structure.

PACS numbers: 73.21.-b,85.75.-d,73.43.Qt,73.61.Wp

Up-today a magnetic field driving by the current of remote write line realizes the reversal of free ferromagnetic layer in a magnetic random access memory (MRAM). The giant magnetoresistance (GMR) effect is used to perform the reading in the storage stripe that is separated from word lines writing the bits¹ or integrated with reading channel.² Along with MRAM the programmable logic can be designed on basis of the GMR effect that utilizes high enough magnetic fields created by the current through a programming line.³ A programmable computing can be realized in such structures as a result of interplay between magnetic fields of input lines affected top and bottom ferromagnetic FM layers with different coercive fields.⁴

Some advantage in device scaling has another mechanism of the MRAM switching based on spin transfer (or spin-torque)^{5,6} in pillar structures.^{7,8} It was demonstrated that spin-polarized current through the magnetic tunnel junction can drive the magnetic switching in nanoscale device.⁹ Note that both aforementioned mechanisms of magnetization reversal need in high critical switching current and consequently high energy dissipation accompanied device operation. Design and creation of a composite free FM layer can result in reducing spin transfer current¹⁰ but it is not so radically that waives the problem of large energy consumption.

At the same time several mechanisms, which completely do not relate to electric current for magnetization reversal have been discussed in literature. Magnetization spontaneous reversal when a temperature variation modifies the exchange bias field in the magnetic heterostructures under the external magnetic field was reported in Ref.¹¹. Involving a multiferroic film to the magnetic structure brings about electrical control of exchange bias field, as it has been recently discussed in Ref.¹². Very recently the authors showed that an atomic thin graphite (graphene) placed between two ferromagnetic dielectric layers (FDLs) realizes an indirect exchange interaction between them and this interaction can be easily controlled by applied electrical bias.¹³ As this is a case, it raises a natural question: Can an graphene-incorporated structure accomplish the magnetization reversal of free FDL and how this effect can be utilized in MRAM and logic devices?

In present study we analysis a different approach to the problem of low-power-consuming non-volatile MRAM and logic design that based on the unique properties of the graphene placed in interface between two magnetic dielectric layers. In particular, the structure under consideration consists of a three ferromagnetic dielectric layers (FDLs) constructed from

same material, which are coupled through monolayer graphene (MG) and bilayer graphene (BG) (Fig. 1). The magnetization of the bottom (\mathbf{M}_b) and top (\mathbf{M}_t) FDLs is pinned by strong enough coercivity or proximate antiferromagnets in the usual fashion.¹⁴ By technology reason they are assumed to be possessed the common direction along x axis so that $\mathbf{M}_b = \mathbf{M}_t \equiv \mathbf{M}_0$. The magnetization \mathbf{M}_f of the middle FDL can be controlled by exchange bias fields mediated by monolayer (\mathbf{H}_1) and bilayer (\mathbf{H}_2) graphenes if their sum exceeds the coercivity of free FDL.

The origin of the \mathbf{H}_1 and \mathbf{H}_2 stems from the exchange interactions $\alpha\mathbf{M}_0\mathbf{S}$ and $\alpha\mathbf{M}_f\mathbf{S}$ of graphene electrons with both pinned \mathbf{M}_0 and free \mathbf{M}_f FDLs (coefficient α is proportional to electron-magnetic ion exchange integral, \mathbf{S} is an electron spin). This establishes an indirect interaction through the graphene electrons in form of Zeeman energy $-\mathbf{H}_n\mathbf{M}_f$ ($n = 1, 2$).¹³

In very general way the thermodynamic potential Ω_n of the graphene electrons interacted with both proximate FDLs determines the effective magnetic field $\mathbf{H}_n = -\partial\Omega_n/\partial\mathbf{M}_f$. Straightforward calculations show that $\mathbf{H}_n \parallel \mathbf{M}_0$ while the effective field projection on this direction $H_n = \mathbf{H}_n\mathbf{M}_0/|\mathbf{M}_0|$ is proportional to the modulation crest of the Ω_n calculated for the electrons exchange interacted with proximate FDLs with parallel, $\Omega_n^{(+)} = \Omega_n|_{\mathbf{M}_f=\mathbf{M}_0}$, and antiparallel, $\Omega_n^{(-)} = \Omega_n|_{\mathbf{M}_f=-\mathbf{M}_0}$ magnetization. Finally it can be shown¹³ that

$$H_n = \frac{\Delta\Omega_n}{2\mathcal{M}_f}, \quad (1)$$

where $\Delta\Omega_n = \Omega_n^{(-)} - \Omega_n^{(+)}$, $\mathcal{M}_f = M_f A_f t_f$ is a total magnetic moment of the free FDL, A_f and t_f are its area and thickness. As in the case of conventional exchange bias, the strength of H_n is inversely proportional to the thickness t_f .¹⁴ This means that the influence of a back magnetic field generated by free DFL on the top and bottom magnetic layers can be strictly weaker their coercive fields under appropriate ferromagnetic layers widths.

The dependence of H_n [Eq. (1)] on the electronic properties of the graphene layer leads to qualitatively different characteristics for MG and BG that the calculation of $\Delta\Omega_1$ and $\Delta\Omega_2$ highlights. In particular the carrier concentration (or position of the electro-chemical potential μ) variation by impurity doping or/and the gate bias (V_{g1} , V_{g2} ; see Fig. 1) significantly influences exchange bias field in different manner for MG and BG.

Firstly, the signs of H_1 and H_2 are different in the wide range μ . While MG tends to establish \mathbf{M}_f parallel to \mathbf{M}_0 ($H_1 > 0$), BG favors the antiparallel alignment ($H_2 < 0$). Secondly, a shift of μ from the graphene i-type point ($\mu = 0$) affects the strengths of the

exchange bias fields \mathbf{H}_1 and \mathbf{H}_2 in the opposite directions. Namely, the magnitude of H_1 gradually increases with $|\mu|$ or electron/hole concentration, whereas that of $|H_2|$ is at the maximum at $\mu = 0$ with minimal free carrier concentration and decreases to zero when $|\mu|$ is large enough. The aforementioned characteristics can be captured by an expression in terms of dimensionless electron exchange energy $G = \alpha M_0 / \gamma_1$ ($\gamma_1 = 0.4$ eV) and the factor $f_n(\mu)$, which provides the specific dependence on μ for MLG ($n = 1$) and BLG ($n = 2$),

$$\Delta\Omega_n = \frac{A_F}{a_g} G^2 f_n(\mu), \quad (2)$$

where $a_g = 0.0537$ nm² is the area of graphene primitive cells. Hereinafter the temperature assumes to be 300 K.

Figure 2 shows the $f_1(\mu)$, $f_2(\mu)$ and their sum vs. $|\mu|$ evaluated at room temperature. As evident from the figure, the shift of $\mu \simeq \pm 0.15\gamma_1$ can change the strength of H_n by about a factor of two for both cases mediated by MG and BG. Moreover, the total field strength $H_1 + H_2 \propto f_1(\mu) + f_2(\mu)$ that controls the magnetization of free FDL varies with μ from negative maximal magnitude through zero to positive value of similar strength provided the μ equality for both MG and BG. The strength of H_n has been estimated at actual μ and $G = 0.1$ as h/t_f , where $h \approx 1000$ Oe·nm.¹³ Such behavior inspires to use the joint action of H_1 and H_2 for electrical switching of free FDL between two stable states, which correspond to \mathbf{M}_f parallel or antiparallel to \mathbf{M}_0 . By analogy with a magnetoresistive memory based on the "spin-valve" effect,^{2,16} we explore the coercivity H_c that secures the stability of the magnetization with respect to quantum and thermal fluctuations. Apparently the strength of coercive magnetic field must be limited by inequality $H_c < h/t_f$. Indeed, in such a case there is a range of exchange bias fields which, guarantees the reversal of magnetization \mathbf{M}_f while \mathbf{M}_0 remains with former orientation.

The Fig. 2 also shows that the neutral charge point can correspond to the effective fields compensation, $H_1 + H_2 = 0$, if the equal impurity doping of MG and BG with magnitude $\mu_0 = 0.11\gamma_1$ has been achieved. Starting with this point, the total field can be variable in both directions by depletion of free carriers or their extra population with electro-chemical potential variation by applied electrical bias of both polarity. Hereinafter the properly impurity doping is assumed to be done for both graphene layers.

Once the problem of \mathbf{M}_f switching between two states $\mathbf{M}_f = \mathbf{M}_0$ and $\mathbf{M}_f = -\mathbf{M}_0$ has been solved, it can be utilized in non-volatile memory provided different magnetic states

of \mathbf{M}_f are surely discerned with graphene electrical properties. As it was recently shown, the conductivity of BG is characterized by significant sensitivity with respect to magnetic ordering of proximate FDLs because an misalignment of \mathbf{M}_f and \mathbf{M}_0 results in bandgap opening and dispersion law flattening.¹⁵ Other possibility consists in magnetic state detection through the MG electronic properties. As in the case of BG, one can expect the higher conductivity in parallel configuration than that in antiparallel orientation. This is because band spin splitting at $\mathbf{M}_f = \mathbf{M}_0$ makes a finite electronic density of states at any electron energy including Dirac point while this is not a case when graphene electrons do not experience spin splitting at $\mathbf{M}_f = -\mathbf{M}_0$. We calculate magnetoresistance of MG and compare it with that for BG at Fig.3. The figure indicates some advantage of BG with respect to magnetoresistance of MG that has been depicted in device design (Fig. 1) with a BG reading line.

At large enough negative $\Delta\mu \equiv \mu - \mu_0 = \Delta\mu_1$ (Fig.4a) graphene-mediated field $|H_1 + H_2|$ exceeds the H_c and turns \mathbf{M}_f opposite to \mathbf{M}_0 direction (Fig. 4b), i.e. their magnetization is antiparallel. Such configuration corresponds to large graphene resistance R_1 (Fig.4c).¹⁵ Such a state remains since the electrical biases will switch off (Fig.4d). As soon as the chemical potentials of both graphene layers supplies the positive magnitude $\Delta\mu \rightarrow \Delta\mu_2$, the \mathbf{M}_f flips toward \mathbf{M}_0 direction (Fig. 4b) so that parallel configuration of the \mathbf{M}_1 and \mathbf{M}_2 results in small graphene resistance R_2 (Fig.4c). Finally, the magnetoresistance reveals a hysteresis loop (Fig. 4d) with electro-chemical potential variation.

An evident advantage of the proposed concept consists in extremely low energy consumption since the graphene electrical recharging during the writing bit does not accompanied by high-density electric current. The intrinsic dissipation energy for each bit recording can be readily estimated in terms of the Eq. (2) as $\Delta W = wA_f$, where $w \approx 3 \cdot 10^{-17}$ J/ μm^2 . Thus, the energy consumption around few 10^{-19} J can be reached as soon as device will be scaling up to lateral sizes of hundred nanometers.

Another potentially useful properties of the device under consideration can be disclosed when one independently manipulates the chemical potentials of MG and/or BG. As a result, the interplay between MG exchange bias field H_1 and BG field H_2 will control the magnetic state of free FDL. In turn, this leads to realization of programmable logic operations AND or OR using V_1 and V_2 as the logic inputs A and B which correspond to be Boolean 0 (1) for negative (positive) voltage. We stress that the design of such logic device is same as the

memory structure. Apparently, the output may be also a voltage related with the resistance of reading channel. We settle the correspondence of high (low) graphene resistance to 0 (1) output.

To demonstrate the device capability to logic operation, we start with antiparallel orientation $\mathbf{M}_f = -\mathbf{M}_0$ (output 0) that can be established after negative pulses applied to both input, i. e. $A = 0$ and $B = 0$. It can be readily show that any combination of the inputs with positive and negative pulses (or $A = 1(0)$ and $B = 1(0)$) generates the magnetic fields H_1 and H_2 which almost compensate each other, i.e. $H_1 + H_2 < H_c$. Hence the output remains 0 for inputs $A = 1, B = 0$ or $A = 0, B = 1$. The only input $A = 1$ and $B = 1$ gives rise constructive field interference $H_1 + H_2 > H_c$ that reverses free FDL in parallel configuration $\mathbf{M}_f = \mathbf{M}_0$ with output 1. (Fig. 5, left panel). Apparently, such input logicity corresponds to operation AND.

If we start with parallel orientation, $\mathbf{M}_f = \mathbf{M}_0$, the output remains 1 under inputs $A = 1, B = 0$ or $A = 0, B = 1$ by same reason of destructive interference of H_1 and H_2 . The only input $A = 0$ and $B = 0$ reverses \mathbf{M}_f that gives rise output 0. (Fig. 5, right panel). Such input pulses logicity results in operation OR.

Fig. 6 recapitulates the programmable logic functioning. Note that the programming pulses precede each input signals, while the datum of logic operation is nonvolatile. Besides the estimation of energy consumption we provided for memory bit recording is applicable to logic as well. Thereby the logic functioning mediated by graphene possesses an advantage of low energy consumption compared with conventional programmable logic using giant magnetoresistance devices.³

In conclusion, we demonstrated that interference of the effective exchange bias fields mediated by the MG and BG enables to provoke the free FDL reversal under electrical bias manipulation. It was also shown that this effect conjointly with graphene giant magnetoresistance can be applied in memory as well as in programmable logic devices with record low energy consumption.

This work was supported in part by the US Army Research Office and the FCRP Center on Functional Engineered Nano Architectonics (FENA).

-
- ¹ D. D. Tang, P. K. Wang, V. S. Speriosu, S. Le, K. K. Kung, *IEEE Trans. Magn.* **31**, 3206, 1995.
 - ² L. V. Melo, L. M. Rodrigues, and P. P. Freitas, *IEEE Trans. Magn.* **33**, 3295, 1997.
 - ³ W. C. Black and B. Das, *J. Appl. Phys.* **87**, 6674 (2000).
 - ⁴ A. Ney, C. Pampuch, R. Koch, and K. H. Ploog, *Nature* **425**, 485 (2003).
 - ⁵ J. C. Slonczewski, *J. Magn. Magn. Mater.* **159**, L1 (1996).
 - ⁶ L. Berger, *Phys. Rev. B* **54**, 9353 (1996).
 - ⁷ J. A. Katine, F. J. Albert, R. A. Buhrman, E. M. Myers, and D. C. Ralph, *Phys. Rev. Lett.* **89**, 3149 (2000).
 - ⁸ Y. Jiang, S. Abe, T. Ochiai, T. Nozaki, A. Hirohata, N. Tezuka, and K. Inomara, *Phys. Rev. Lett.* **92**, 167204 (2004).
 - ⁹ G. D. Fuchs, N. C. Emley, I. N. Krivorotov, P. M. Braganca, E. M. Ryan, S. I. Kiselev, J. C. Sankey, D. C. Ralph, and R. A. Burhman, *Appl. Phys. Lett.* **85**, 1205 (2004).
 - ¹⁰ H. Meng and J.-P. Wang, *Appl. Phys. Lett.* **89**, 152509 (2006).
 - ¹¹ Z. P. Li, J. Eisenmenger, C. W. Miller, and I. K. Schuller, *Phys. Rev. Lett.* **96**, 137201 (2006).
 - ¹² H. Béa, M. Bibes, F. Ott, B. Dupé, X.-H. Zhu, S. Petit, S. Fusil, C. Deranlot, K. Bouzehouane, and A. Bartélémy, *Phys. Rev. Lett.* **100**, 017204 (2008).
 - ¹³ Y. G. Semenov, J. M. Zavada, and K. W. Kim, *Phys. Rev. Lett.* **101**, 147206 (2008).
 - ¹⁴ J. Nogués and I. K. Schuller, *J. Magn. Magn. Mater.* **192**, 203 (1999).
 - ¹⁵ Y. G. Semenov, J. M. Zavada, and K. W. Kim, *Phys. Rev. B* **77**, 235415 (2008).
 - ¹⁶ K. Matsuyama, H. Asada, S. Ikeda, and K. Taniguchi, *IEEE Trans. Magn.* **33**, 3283 (1997).

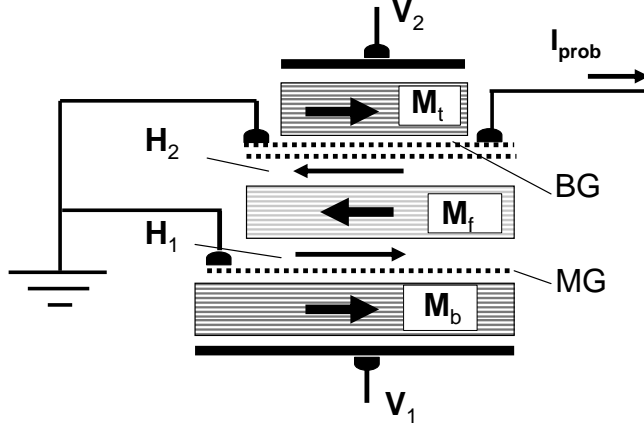


FIG. 1: Schematic illustration of the free DFL with magnetization \mathbf{M}_f (thick arrow) sandwiched between MG and BG, which mediate exchange bias fields \mathbf{H}_1 and \mathbf{H}_2 correspondingly (thin arrows). The strengths and directions of these fields control two other DFLs placed at the top (magnetization \mathbf{M}_t) and bottom (magnetization \mathbf{M}_b) of the structure. In turn, the \mathbf{M}_t and \mathbf{M}_b are pinned by relatively strong coercivity or proximate antiferromagnets (does not shown). The voltages V_1 and V_2 control the electrical bias; the prob current I_{prob} indicates magnetoresistance.

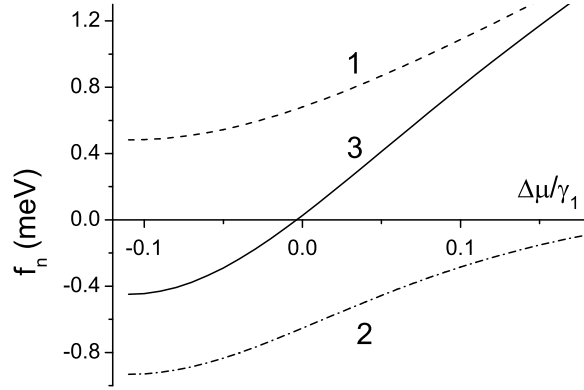


FIG. 2: Factors $f_n(\mu, T) = \Delta\Omega_n(\pi)/NG^2$, $n=1,2$, (curves 1 and 2) and their sum (curve 3), which determines the exchange bias field variation with electro-chemical potential shift for both MLG ($\Delta\Omega_1(\pi) > 0$) and BLG ($\Delta\Omega_2(\pi) < 0$).

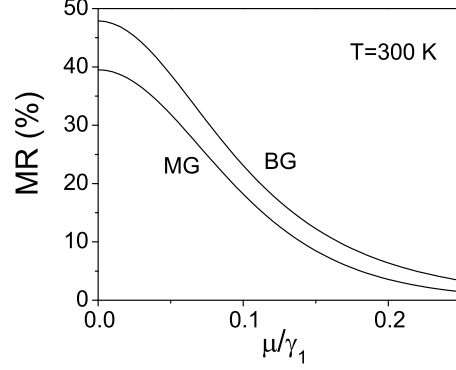


FIG. 3: Magnetoresistance of MLG and BLG vs. electro-chemical potential calculated at room temperature.

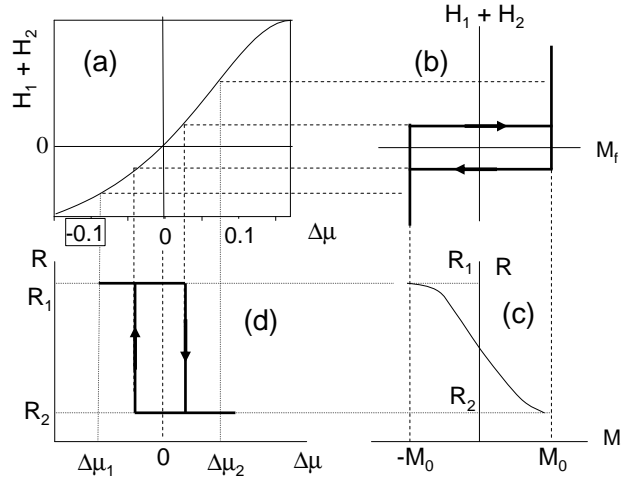


FIG. 4: Schematic diagram illustrating the origin of electrical bistability of the structure. (a) The effective field mediated at the top FDL by the sum of MLG field H_1 and BLG field H_2 as a function of electro-chemical potential shift $\Delta\mu = \mu - \mu_0$. μ_1 and μ_2 cause the effective fields stronger the coercivity, hence they provoke flips of M_f . (b) Hysteresis loop of magnetization M_f in the effective field variable by $\Delta\mu$. (c) the curve of magnetoresistance versus magnetization M_f controlled by $\Delta\mu$ shift. (d) Magnetoresistance loop with $\Delta\mu$ variation: $\Delta\mu = 0$ corresponds to high (R_1) or low (R_2) graphene resistance, alteration between $\Delta\mu_1$ and $\Delta\mu_2$ executes the switching between these states

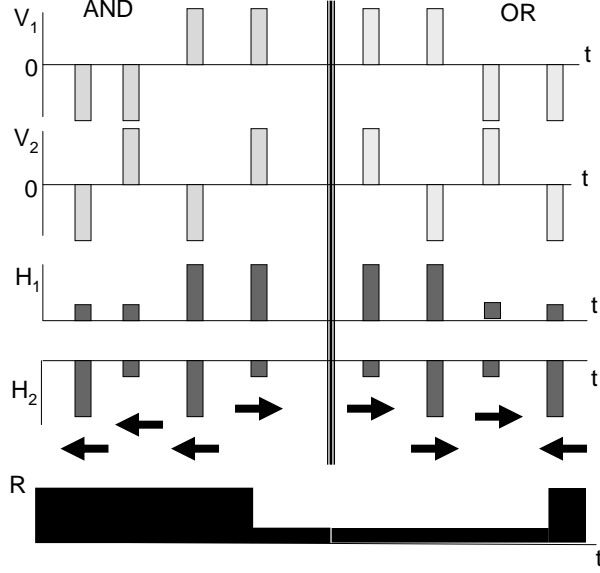


FIG. 5: Diagram of logic operation AND (left panel) and OR (right panel). Input voltages V_1 and V_2 control exchange bias fields H_1 and H_2 so that voltages of different sign mediate magnetic fields of opposite directions that almost compensate each other. Arrows indicate the stable directions of free FDL magnetization parallel (right-directed) or antiparallel (left-directed) to \mathbf{M}_0 . The R shows variation of magnetoresistance, which corresponds to current magnetization directions.

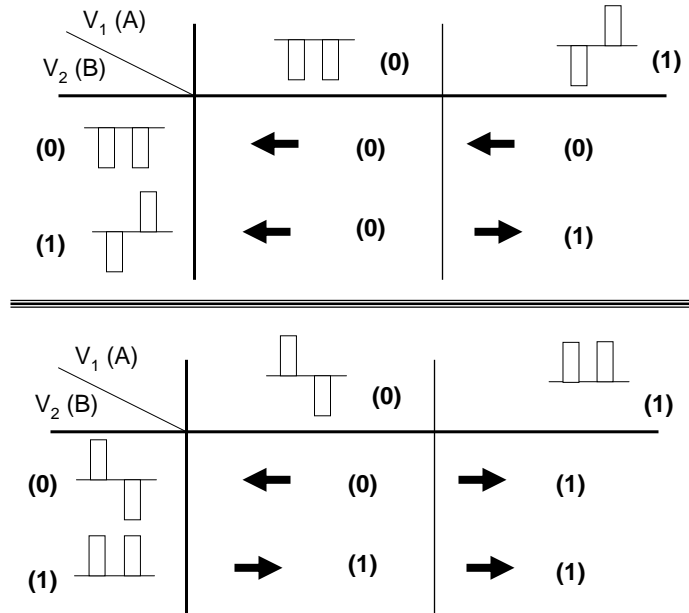


FIG. 6: The magnetization states of free ferromagnetic layer and corresponded Boolean variables after programming pulses AND (top part) and OR (bottom part) and different combination of input $A = 0, 1$ and $B = 0, 1$.